



Tuning energy transfer efficiency in quantum dots mixture by controlling donor/acceptor ratio

Chang Liu(刘畅), Jing Liang(梁晶), Fangfang Wang(王芳芳), Chaojie Ma(马超杰), Kehai Liu(刘科海), Can Liu(刘灿), Hao Hong(洪浩), Huaibin Shen(申怀彬), Kaihui Liu(刘开辉), and Enge Wang(王恩哥)

Citation: Chin. Phys. B, 2021, 30 (12): 127802. DOI: 10.1088/1674-1056/ac29b2

Journal homepage: <http://cpb.iphy.ac.cn>; <http://iopscience.iop.org/cpb>

What follows is a list of articles you may be interested in

Investigation of fluorescence resonance energy transfer ultrafast dynamics in electrostatically repulsed and attracted exciton-plasmon systems

Hong-Yu Tu(屠宏宇), Ji-Chao Cheng(程基超), Gen-Cai Pan(潘根才), Lu Han(韩露), Bin Duan(段彬), Hai-Yu Wang(王海宇), Qi-Dai Chen(陈岐岱), Shu-Ping Xu(徐抒平), Zhen-Wen Dai(戴振文), and Ling-Yun Pan(潘凌云)

Chin. Phys. B, 2021, 30 (2): 027802. DOI: 10.1088/1674-1056/abb802

The effects of Er^{3+} ion concentration on 2.0- μm emission performance in $\text{Ho}^{3+}/\text{Tm}^{3+}$ co-doped $\text{Na}_5\text{Y}_9\text{F}_{32}$ single crystal under 800-nm excitation

Benli Ding(丁本利), Xiong Zhou(周雄), Jianli Zhang(章践立), Haiping Xia(夏海平), Hongwei Song(宋宏伟), and Baojiu Chen(陈宝玖)

Chin. Phys. B, 2021, 30 (1): 017801. DOI: 10.1088/1674-1056/abaede

Cascaded plasmonic nanorod antenna for large broadband local electric field enhancement

Dou Zhang(张豆), Zhong-Jian Yang(杨中见), Jun He(何军)

Chin. Phys. B, 2019, 28 (10): 107802. DOI: 10.1088/1674-1056/ab3f99

Substitution priority of Eu^{2+} in multi-cation compound $\text{Sr}_{0.8}\text{Ca}_{0.2}\text{Al}_2\text{Si}_2\text{O}_8$ and energy transfer

Zhi-Ping Yang(杨志平), Zhen-Ling Li(李振玲), Zhi-Jun Wang(王志军), Pan-Lai Li(李盼来), Miao-Miao Tian(田苗苗), Jin-Ge Cheng(程金阁), Chao Wang(王超)

Chin. Phys. B, 2018, 27 (1): 017802. DOI: 10.1088/1674-1056/27/1/017802

2.0- μm emission and energy transfer of $\text{Ho}^{3+}/\text{Yb}^{3+}$ co-doped LiYF_4 single crystal excited by 980 nm

Yang Shuo, Xia Hai-Ping, Jiang Yong-Zhang, Zhang Jia-Zhong, Jiang Dong-Sheng, Wang Cheng, Feng Zhi-Gang, Zhang Jian, Gu Xue-Mei, Zhang Jian-Li, Jiang Hao-Chuan, Chen Bao-Jiu

Chin. Phys. B, 2015, 24 (6): 067802. DOI: 10.1088/1674-1056/24/6/067802

Tuning energy transfer efficiency in quantum dots mixture by controlling donor/acceptor ratio*

Chang Liu(刘畅)^{1,†}, Jing Liang(梁晶)^{2,†}, Fangfang Wang(王芳芳)^{3,†}, Chaojie Ma(马超杰)²,
Kehai Liu(刘科海)⁴, Can Liu(刘灿)², Hao Hong(洪浩)^{2,¶},
Huaibin Shen(申怀彬)^{3,§}, Kaihui Liu(刘开辉)^{1,2,‡}, and Enge Wang(王恩哥)^{1,4}

¹International Centre for Quantum Materials, Collaborative Innovation Centre of Quantum Matter, Peking University, Beijing 100871, China

²State Key Laboratory for Mesoscopic Physics, Frontiers Science Center for Nano-optoelectronics, School of Physics, Peking University, Beijing 100871, China

³Key Laboratory for Special Functional Materials of Ministry of Education, School of Materials and Engineering, Henan University, Kaifeng 475001, China

⁴Songshan Lake Materials Laboratory, Institute of Physics, Chinese Academy of Sciences, Dongguan 523000, China

(Received 15 August 2021; revised manuscript received 10 September 2021; accepted manuscript online 24 September 2021)

Improving the emission performance of colloidal quantum dots (QDs) is of paramount importance for their applications on light-emitting diodes (LEDs), displays and lasers. A highly promising approach is to tune the carrier recombination channels and lifetime by exploiting the energy transfer process. However, to achieve this precise emission optimization, quantitative modulation on energy transfer efficiency is highly desirable but still challenging. Here, we demonstrate a convenient approach to realize tunable energy transfer efficiency by forming QDs mixture with controllable donor/acceptor (D/A) ratio. With the mixing ratio ranging from 16/1 to 1/16, the energy transfer efficiency could be effectively tuned from near zero to $\sim 70\%$. For the high mixing ratio of 16/1, acceptors obtain adequate energy supplied by closely surrounding donors, leading to ~ 2.4 -fold PL enhancement. While for the low mixing ratio, the ultrafast and efficient energy extraction process directly suppresses the multi-exciton and Auger recombination in the donor, bringing about a higher threshold. The facile modulation of emission performance by controllably designed mixing ratio and quantitatively tunable energy transfer efficiency will facilitate QD-based optoelectronic and photovoltaic applications.

Keywords: colloidal quantum dots, energy transfer, emission engineering, Auger suppression

PACS: 78.67.-n, 78.67.Hc

DOI: 10.1088/1674-1056/ac29b2

Colloidal quantum dots (QDs) are quantum-confined semiconductor nanocrystals with high absorption, near-unity photoluminescence (PL) quantum yield, narrow emission linewidth and high photostability.^[1–3] Those admirable merits, together with the convenience of tuning bandgap and surface functionalization, promote the boom of QD-based electronic and optoelectronic devices with low-cost solution-based fabrication procedure, including QD light-emitting diodes (QLEDs), displays and lasing devices.^[4–9] To improve the emission performances and meet the specific needs of applications, various methods have been widely developed by optimizing the materials synthesis and device architecture,^[9–11] such as synthesis of QDs with core-shell structure^[12–14] and adoption of hybrid organic/inorganic charge transport layers.^[15,16] With those improvements, QLEDs have experienced a rapid growth in their external quantum efficiency (EQE). In addition, white QLEDs (WQLEDs) with different

structures have also been developed, such as mixing blue, green and red QDs together in the emitting layer^[17,18] or depositing different emitting layers separately.^[19–21] Due to the close vicinity of QDs, those mixed or multi-layered WQLEDs suffer from energy loss due to the down conversion energy transfer process and defect quenching. Non-radiative Auger recombination can also result in energy loss and lower EQE in both QLEDs and WQLEDs under high carrier density. Therefore, a simple, convenient but sufficient approach to further improve the emission performances is highly desirable but still waiting for deep exploration.

Förster resonance energy transfer process, which describes nonradiative energy transfer via dipole–dipole coupling from a fluorescent donor to a proximal acceptor with spectral overlap,^[22–27] exhibits powerful modulation effects on the emission performance of QDs.^[28–38] With the energy flow from donor to acceptor, both the absorption and emission

*Project supported by the National Natural Science Foundation of China (Grant Nos. 52025023, 51991342, 52021006, 11888101, and 61922028), the Key R&D Program of Guangdong Province, China (Grant Nos. 2020B010189001, 2019B010931001, and 2018B030327001), the Strategic Priority Research Program of Chinese Academy of Sciences (Grant No. XDB33000000), Beijing Natural Science Foundation, China (Grant No. JQ19004), the Pearl River Talent Recruitment Program of Guangdong Province, China (Grant No. 2019ZT08C321), and China Postdoctoral Science Foundation (Grant No. 2021T140022).

† These authors contributed equally to this work.

‡ Corresponding author. E-mail: khliu@pku.edu.cn

§ Corresponding author. E-mail: shenhuaibin@henu.edu.cn

¶ Corresponding author. E-mail: haohong@pku.edu.cn

properties of QDs could be effectively regulated, such as absorption cross section, carrier lifetime and PL intensity. The energy transfer efficiency between donor and acceptor can be directly modulated by the separation distance, spectral overlap as well as the number of interacting donor and acceptor. Exploring the energy transfer process will benefit for better controlling and designing artificial QDs systems with configurable optoelectronic properties. Significantly, quantitative modulation on energy transfer efficiency is highly demanded to realize such precise optimization of QDs performances.

In this work, we have realized tunable energy transfer efficiency by forming QDs mixtures with controllable mixing ratio. By carefully mixing up the donor and acceptor QDs with appropriate donor/acceptor (D/A) ratio (Fig. 1(a)), the energy transfer efficiency can be tuned from near zero to $\sim 70\%$. The modulation of energy transfer efficiency and carrier dynamics channels in the mixture will naturally tune the emission properties of both donor and acceptor, where enlarged absorption cross section leads to enhanced emission intensity for the acceptor and the sufficient energy extraction in donor will suppress the multi-exciton and non-radiative Auger recombination.

Realization of energy transfer in QDs mixtures. In our experiments, high quality core/shell CdSe/ZnS QDs were

fabricated by high temperature hot-injection strategy (Fig. S1 showing the energy band diagram of core/shell CdSe/ZnS QDs). By adjusting the ratios of precursor and the reaction time, the core size and the corresponding bandgap were artificially tuned from 500 nm to 650 nm continuously (see Appendix A for details).^[39] Here, the fabricated QDs with emission spectra centered at 532 nm and 620 nm were used as donor and acceptor, respectively, as shown in Figs. 1(b) and 1(c). Ultraviolet photoelectron spectroscopy (UPS) and energy level of QDs can be found in Fig. S2. These two QDs were mixed up in solution with appropriate ratio and deposited onto the 300 nm SiO₂/Si substrate by spin coating. The PL spectra of both pure QDs and the mixture are shown in Fig. 1(d), where the PL intensity in mixture has been normalized with respect to the concentration of pure QDs to make meaningful comparison. From the spectra, we can find the suppressed PL intensity from the donor and enhanced intensity from the acceptor in the mixture (1/1), due to the energy transfer process. According to the modulation of the PL intensity, the energy transfer efficiency η can be directly determined as $\eta = 1 - I_{DA}/I_D$, where I_D is the PL intensity from pure donor and I_{DA} is the PL intensity from donor in the mixture. For the mixture (1/1) studied here, the energy transfer efficiency η is given as $\sim 28\%$.

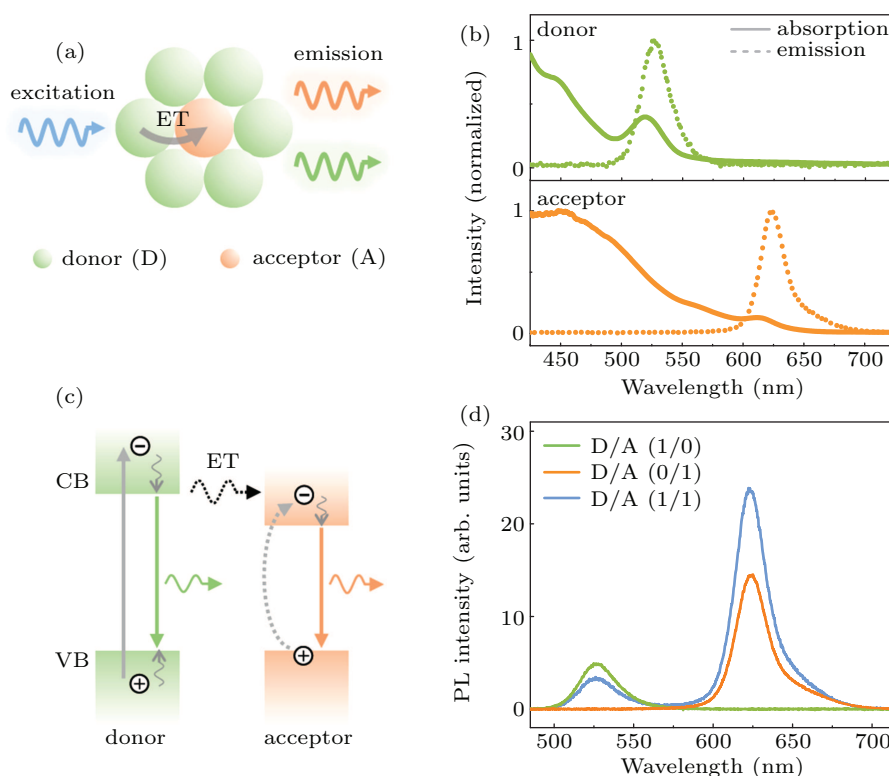


Fig. 1. Energy transfer in the QDs mixture. (a) Schematic representation of QDs mixture under laser excitation. Energy transfer (ET) takes place between two kinds of QDs with spectral overlap in proximity to each other, which influences their PL intensity and PL decay dynamics. (b) Absorption (solid line) and emission (dashed line) spectra of donor and acceptor QDs. The obvious spectral overlap of donor's emission and acceptor's absorption spectra promises the efficient energy transfer. (c) Schematic band diagram of donor and acceptor QDs. With non-radiative energy transfer, the exciton generated in donor undergoes energy transfer process into absorbing states of acceptor. (d) PL intensity of pure donor (olive), pure acceptor (orange) and mixture (1/1) (blue) under the same excitation condition. The PL intensity in mixture has been normalized with respect to the concentration of pure QDs. The enhanced PL of acceptor and suppressed PL of donor indicate efficient energy transfer between them.

Tunable energy transfer efficiency in QDs mixtures.

The naturally existing energy transfer process in QDs mixtures effectively influences the emission performances of both donor and acceptor. In order to modulate the energy transfer efficiency, QDs mixtures with different D/A ratio were prepared and studied. Pulse laser from Ti: sapphire oscillator (250 kHz, 60 fs) centered at 400 nm was used to characterize the time-resolved optical spectra. After photoexcitation, the emission signals were collected by a microscope objective and sent to our detection system to characterize the PL dynamics for both donor and acceptor (see Appendix A and Fig. S3 for details). With the increase of the acceptor proportion, the donor lifetime was shortened gradually (Fig. 2(a)). As in mixture (1/16), the donor lifetime was fitted to be ~ 1.4 ns, much shorter than the pure donor lifetime of ~ 4.4 ns (Fig. 2(c) and Table S1). Meanwhile, the lifetime of acceptor became longer in the mixture (Fig. 2(b)). With the increase of the donor proportion, the acceptor lifetime gradually approached the maximum value, indicating the saturation of the energy transfer process (Fig. 2(c)). Lifetime modulation for donor and acceptor in the mixtures has exhibited opposite trends, implying

the directional energy flow from donor to acceptor. The effective energy transfer time can be derived from the formula $\frac{1}{\tau_{ET}} = \frac{\tau_D - \tau_{DA}}{\tau_D \tau_{DA}}$, where τ_{ET} is the time constant of energy transfer, τ_D is the lifetime of pure donor and τ_{DA} is the lifetime of donor in the mixture (Tables S1 and S2). The effective energy transfer time in mixture (1/16) can be obtained as $\tau_{ET} \sim 2.0$ ns, revealing the competing fast non-radiative energy transfer decay channel. Considering the formula of the effective energy transfer rate, $\Gamma_{DA} = \frac{1}{\tau_{ET}} = \frac{1}{\tau_0} \frac{R_0^6}{R_{DA}^6}$, the Förster radius R_0 thus can be derived to be about ~ 12.5 nm, where the Förster radius describes the distance between donor and acceptor for energy transfer efficiency of 50%, R_{DA} is the distance between donor and acceptor (about ~ 11 nm, containing the radius of donor and acceptor QDs with oleic acid ligand) and τ_0 is the lifetime of donor excited states. Transmission electron microscope images showing the size of both donor and acceptor can be found in Fig. S4. In our experiment, the size of donor is ~ 8.5 nm with 4 monolayer (ML) ZnS, and the size of acceptor is ~ 10.5 nm with 3 ML ZnS. Each ML of ZnS is about 0.31 nm.

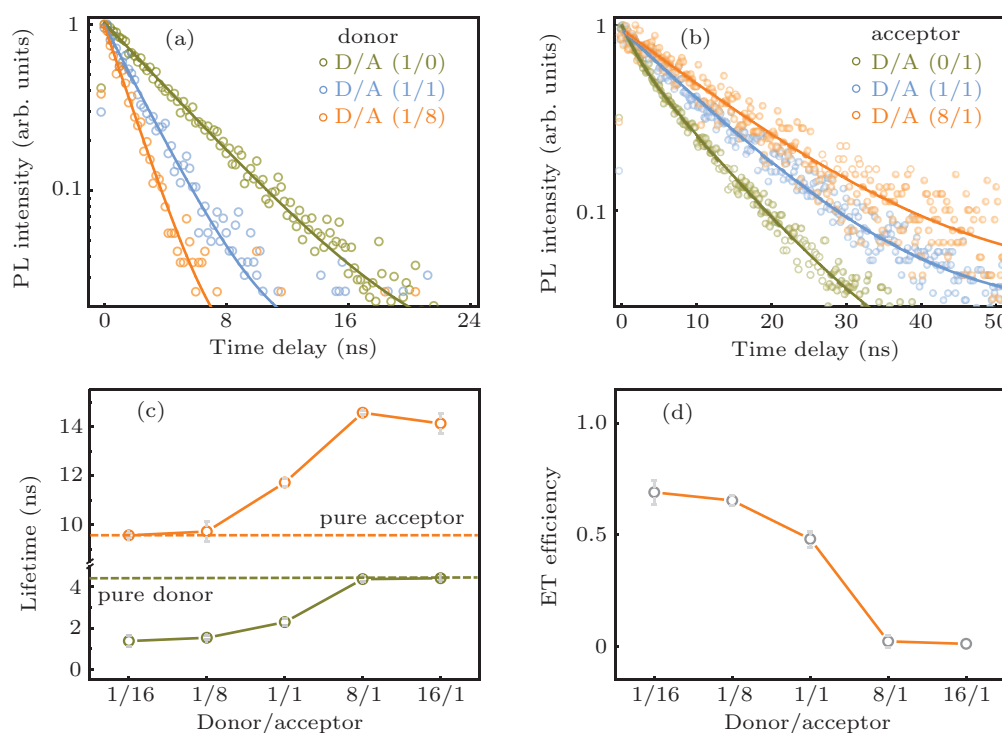


Fig. 2. Lifetime modulation of donor and acceptor in the mixture. (a), (b) PL decay dynamics of donor (a) and acceptor (b) in the mixture with different mixing ratio. (c) Lifetime statistics extracted from the PL decay curves. The orange/olive dashed lines represent the lifetime of pure acceptor/donor, respectively. (d) Energy transfer (ET) efficiency from donor to acceptor in the mixture with different D/A ratio.

The variation of lifetime for donor and acceptor in mixtures with different D/A ratios implied the different modulation effects of energy transfer. Besides the donor PL intensity, the donor lifetime in mixture can also be used to calculate the energy transfer efficiency η , according to the formula $\eta = 1 - \tau_{DA}/\tau_D$, where τ_D is the lifetime of pure donor and τ_{DA} is the lifetime of donor in the mixture. Remark-

ably, the energy transfer efficiency can be tuned from near zero to $\sim 70\%$ by varying the D/A ratio from 16/1 to 1/16 (Fig. 2(d)). Energy transfer process can take place between donor and acceptor in close proximity. The amount of energy transferred into the acceptor is directly influenced by the number of surrounding donors as well as the distance between them, according to the formula of the energy transfer effi-

ciency, $\eta = nR_0^6/(nR_0^6 + R_{DA}^6)$, where n is the number of acceptors interacting with one donor.^[40,41] With the increase of acceptor proportion, donor can be totally surrounded by acceptors (e.g., 1/16), leading to the sufficient energy extraction from donor to acceptor and corresponding high energy transfer efficiency. The simple but precise tuning method for energy transfer efficiency provides us a powerful tool to achieve controllable optimization of emission performance for QDs.

Enhanced PL intensity for acceptor. With external energy transferred from the surrounding donors into acceptor, PL intensity of acceptor can be enhanced in mixtures. In addition to the absorption of the acceptor determined by its intrinsic absorption cross section, extra energy supplement directly increases the total absorption and emission intensity for acceptor (Fig. 3(a)), if the change of the acceptor quantum yield is ignored. Actually, the effective absorption of acceptor (Abs_e)

in mixtures can be expressed as $Abs_e = Abs_D \cdot \eta + Abs_A$, where Abs_D and Abs_A are the absorption of donor and acceptor respectively and η is the energy transfer efficiency between them.^[37] Therefore, the total absorption is influenced by the energy transfer efficiency, which is determined by the D/A ratio in the mixtures. Accordingly, with the increase of the donor proportion, the PL intensity of acceptor in mixtures was enhanced gradually and would approach a maximum value when the energy transfer process approached its saturation (Fig. 3(b)). The PL intensity of acceptor in the mixture (16/1) was enhanced to ~ 2.4 -fold, benefitted from the energy transfer process (Fig. 3(c)). Enlarged effective absorption of acceptor with extra energy supplement from donor results in the emission enhancement of acceptor, which can be precisely controlled by tuning the D/A ratio.

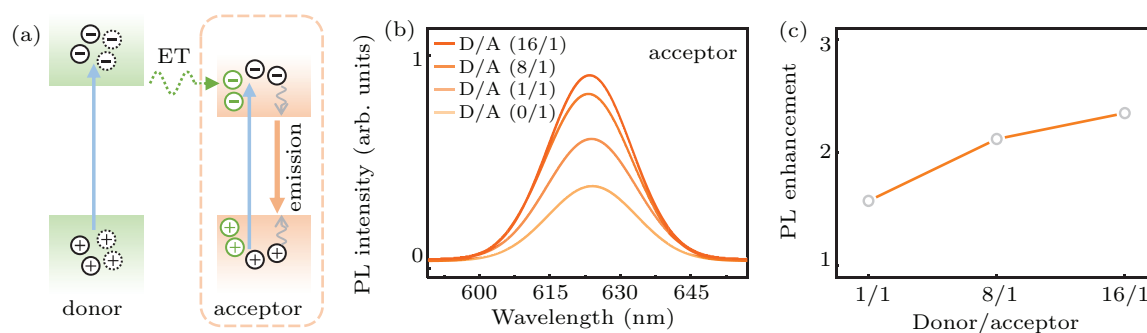


Fig. 3. PL enhancement for acceptor in the mixture. (a) Schematics showing the energy flow from donor to acceptor in the mixture. With more donors surrounding in proximity, the acceptor obtains more energy and thus shows enhanced emission intensity. (b) PL intensity of acceptor in the mixture with different mixing ratio. The PL intensity in mixture has been normalized with respect to the concentration of pure QDs. (c) PL enhancement factor of acceptor in the mixture. With the increase of the donor proportion, the acceptor PL intensity shows an increasing enhancement factor.

Suppressed Auger recombination for donor. Due to the relatively larger size of the exciton Bohr radius than the QDs size, the exciton is confined in the limited volume of nanoparticle. Hence multi-exciton recombination as well as non-radiative Auger recombination process will dominate the emission behavior in the QDs under high carrier density.^[42–46] When the rate of energy transfer is comparable to that of Auger recombination, energy extraction from donor holds the promise of reducing corresponding energy loss (Fig. 4(a)). Lifetime characterization of donor has been carried out to study the recombination channels of donor under different excitation power density. With the increase of the excitation power density, the initial single-exponential decay curve underwent change to multi-exponential decay process for pure donor (Fig. 4(c)). The threshold is approximately 0.02 mJ/cm^2 , above which faster decay channels became apparent. Those faster decays are attributed to the non-exciton recombination channels including charged exciton, multi-exciton and non-radiative Auger recombination process, which are faster than the radiative neutral exciton recombination and result in the PL blinking because of their lower emissivities.^[47–52] However, as for the donor in the mixture

(1/8), no obvious change can be detected in the PL decay traces with the increase of the excitation power (Fig. 4(d)). The PL decay curves of donor in the mixture still show good single-exponential fitting even at higher excitation power (e.g., 0.2 mJ/cm^2), which is not the case for pure donor (Fig. 4(b)). The single-exponential decay curve means that the energy transfer is faster than other decay channels and the emerging Auger recombination process in donor is actually covered by energy transfer under high fluence excitation and strong emission (Fig. S5). Resulted from the reduced exciton concentration, donor in mixtures surrounded with acceptors possess a higher threshold for non-radiative Auger recombination and can continue with the radiative neutral exciton recombination under a higher excitation power density. What is more, the reduced impact of Auger recombination for donor avoids the energy loss of such non-radiative decays, and the energy transported into acceptor further improves the quantum efficiency of acceptor on the other hand. Suppressed Auger recombination in donor and enlarged absorption and emission in acceptor hold the promise to effectively improve the emission performances of WQLEDs.

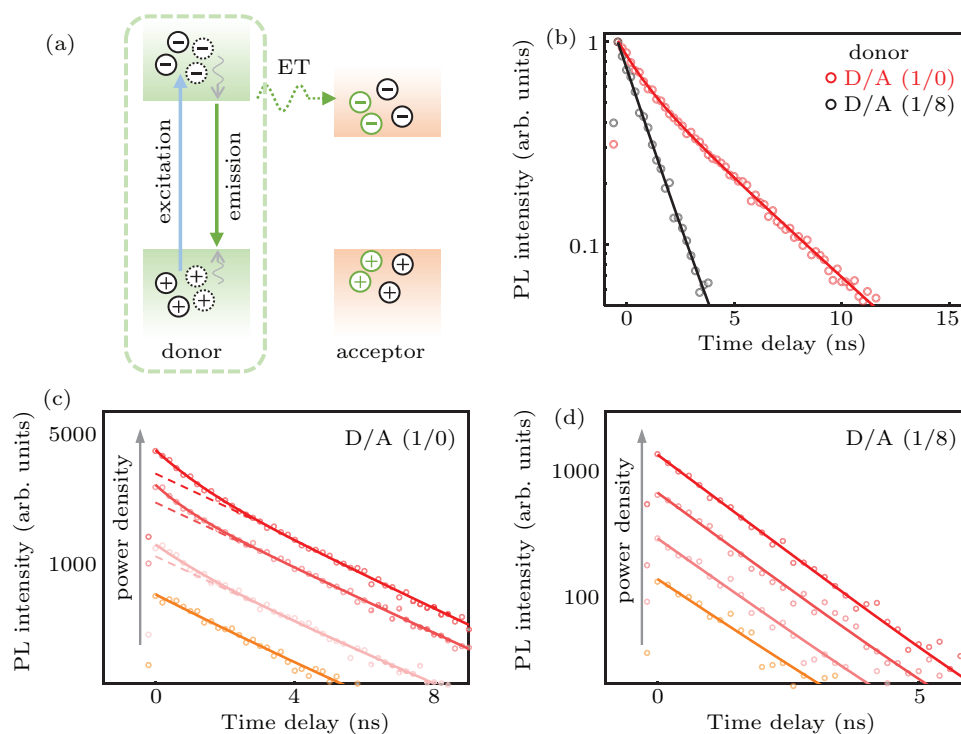


Fig. 4. Suppression of Auger recombination process for donor in the mixture (1/8). (a) Schematics showing exciton extracting process in mixture of QDs between the donor and acceptor. With the efficient energy transfer, the exciton concentration in donor decreases, and so does the non-radiative Auger recombination rate. (b) PL decay dynamics of donor in mixture (black) and pure donor (red) under high excitation power intensity (0.2 mJ/cm^2). Pure donor shows multi-exponential decay process (red), while donor in the mixture still undergoes single-exponential decay. (c), (d) Excitation power-dependent PL decay dynamics of (c) pure donor and (d) donor in mixture (1/8). The excitation power density is 0.01, 0.02, 0.05 and 0.2 mJ/cm^2 , respectively, from bottom to top. Dashed lines in (c) help to highlight the multi-exponential decay process of pure donor even under low excitation power.

Precise optimization of emission performance for QDs can be realized by choosing appropriate D/A ratio by making full use of the tunable energy transfer process. When at high D/A ratio, the directional injection of excitons into acceptors from proximal donors lever up the emission intensity. What is more, the sufficiently enhanced absorption for acceptor could provide extra pumping in the stimulated emission regime and lower corresponding gain threshold potentially, indicating the feasibility of QD-based optical amplifiers and lasers based on energy transfer strategy. As for donor in the mixtures, the ultrafast energy extraction process can make donor tolerate higher fluence excitation and results in a higher threshold for Auger recombination. The quantitatively tunable energy transfer efficiency in mixtures also provides a practical strategy to design and further improve WQLEDs with proper mixing ratio to realize optimized emission performances such as reduced energy loss due to Auger recombination, etc.

In summary, we have successfully realized tunable energy transfer efficiency in QDs system, which can be modulated from near zero to $\sim 70\%$ by controlling the D/A ratio. Taking advantage of the precisely modulated energy transfer process existing in the mixtures, improved emission performance of QDs can be achieved. We believe that the convenient realization of tunable and sufficient energy transfer by forming QDs mixtures with proper D/A ratio provides a powerful tool to precisely optimize the emission performances of

QLEDs as well as WQLEDs. Our results provide a perspective to better understand energy transfer process quantitatively and will promote the utilization of tunable energy transfer to design high-performance QD-based optoelectronic and photovoltaic devices.

Appendix A: Methods

Synthesis of CdSe/ZnS QDs. Cadmium oxide (CdO, 99.99%), sulfur (S, 99.99%, powder), 1-octadecene (ODE, 90%), oleic acid (OA, 90%), selenium (Se, 99.999%, powder), and zinc oxide (ZnO, 99.99%, powder) were purchased from Aldrich. High quality CdSe core and CdSe/ZnS core/shell QDs were synthesized according to our reported procedures.^[39] As for shell precursors, zinc oleate (0.2 M) was prepared by heating a mixture of ZnO (0.4882 g, 6 mmol), oleic acid (5.084 g, 18 mmol), and ODE (24 mL) to 300°C . Sulfur precursor (0.2 M) was prepared by heating a mixture of sulfur (0.192 g, 6 mmol) and ODE (30 mL) to 150°C . By choosing suitable size of CdSe as cores, core/shell QDs with emitting color from green to red have been synthesized. 3 mL of ODE and 1 g of OA were loaded into a 50 mL reaction flask. The purified CdSe QDs in hexanes (2.8 nm and 4.7 nm in diameter) were added, and the system was kept at 120°C under nitrogen flow for 30 min to remove hexanes. Subsequently, the solution was heated from 180°C to 280°C for the shell

growth at a rate of 20 °C per 10 min with adding shell precursors. Finally, the required nanocrystals were dispersed in octane.

Characterization of QDs. Room temperature UV-vis absorption spectra were measured with an Ocean Optics spectrophotometer (mode PC2000-ISA). Transmission electron microscopy (TEM) studies were performed using a JEOL JEM-2010 electron microscope operating at 200 kV.

Sample preparation. Two kinds of colloidal QDs in solution were mixed up with different D/A ratio. The mixed solution was then thoroughly mixed up in the water bath with ultrasonic vibration. The mixture was dropped and spun cast onto the 300 nm SiO₂/Si substrate layer with 3000 r/min rotation speed. The samples of pure donor and acceptor were prepared using the same method to make comparison.

PL and time-resolved PL measurements. All the PL measurements were carried out by using our home-made experimental setup. The samples were excited by the pulse laser centered at 400 nm (Coherent Vitara-T, ~ 60 fs, 250 kHz) generated by a Ti:sapphire oscillator and a BBO crystal. Excitation laser was focused by a Nikon objective (50×, NA ~ 0.80) and the emission signal was collected by the same objective under reflection mode. The collected signal was then sent to the spectrometer (Princeton Instruments) after filtering out the excitation laser to analyse the PL intensity. As for time-resolved PL measurement, the collected signal was sent to the time-correlated single-photon counting system (Picoquant, Timeharp 260).

References

- [1] Murray C B, Kagan C R and Bawendi M G 2000 *Ann. Rev. Mater. Sci.* **30** 545
- [2] Talapin D V, Lee J S, Kovalenko M V and Shevchenko E V 2010 *Chem. Rev.* **110** 389
- [3] Yang J, Choi M K, Kim D H and Hyeon T 2016 *Adv. Mater.* **28** 1176
- [4] Dai X L, Zhang Z X, Jin Y Z, Niu Y, Cao H J, Liang X Y, Chen L W, Wang J P and Peng X G 2014 *Nature* **515** 96
- [5] Fan F J, Wu L and Yu S H 2014 *Energ Environ Sci.* **7** 190
- [6] Kagan C R, Lifshitz E, Sargent E H and Talapin D V 2016 *Science* **353** aac5523
- [7] Siboni H Z, Sadeghimakki B, Sivoththaman S and Aziz H 2015 *Acs Appl. Mater. Inter.* **7** 25828
- [8] Sun Q, Wang Y A, Li L S, Wang D Y, Zhu T, Xu J, Yang C H and Li Y F 2007 *Nat. Photon.* **1** 717
- [9] Litvin A P, Martynenko I V, Purcell-Milton F, Baranov A V, Fedorov A V and Gun'ko Y K 2017 *J. Mater. Chem. A* **5** 13252
- [10] Mashford B S, Stevenson M, Popovic Z, Hamilton C, Zhou Z Q, Breen C, Steckel J, Bulovic V, Bawendi M, Coe-Sullivan S and Kazlas P T 2013 *Nat. Photon.* **7** 407
- [11] Shen H B, Cao W R, Shewmon N T, Yang C C, Li L S and Xue J G 2015 *Nano Lett.* **15** 1211
- [12] Coe S, Woo W K, Bawendi M and Bulovic V 2002 *Nature* **420** 800
- [13] Mattoussi H, Radzilowski L H, Dabbousi B O, Thomas E L, Bawendi M G and Rubner M F 1998 *J. Appl. Phys.* **83** 7965
- [14] Schlamp M C, Peng X G and Alivisatos A P 1997 *J. Appl. Phys.* **82** 5837
- [15] Cho K S, Lee E K, Joo W J, Jang E, Kim T H, Lee S J, Kwon S J, Han J Y, Kim B K, Choi B L and Kim J M 2009 *Nat. Photon.* **3** 341
- [16] Yang Y X, Zheng Y, Cao W R, Titov A, Hyvonen J, Manders J R, Xue J G, Holloway P H and Qian L 2015 *Nat. Photon.* **9** 259
- [17] Bae W K, Lim J, Lee D, Park M, Lee H, Kwak J, Char K, Lee C and Lee S 2014 *Adv. Mater.* **26** 6387
- [18] Lee K H, Han C Y, Kang H D, Ko H, Lee C, Lee J, Myoung N, Yim S Y and Yang H 2015 *Acs Nano* **9** 10941
- [19] Bae W K, Kwak J, Lim J, Lee D, Nam M K, Char K, Lee C and Lee S 2010 *Nano Lett.* **10** 2368
- [20] Jiang C B, Zou J H, Liu Y, Song C, He Z W, Zhong Z J, Wang J, Yip H L, Peng J B and Cao Y 2018 *Acs Nano* **12** 6040
- [21] Zhang H, Su Q, Sun Y Z and Chen S M 2018 *Adv. Opt. Mater.* **6** 1800354
- [22] Förster T 1948 *Ann. Phys.-Berlin* **2** 55
- [23] Lakowicz J R 2013 *Principles of Fluorescence Spectroscopy*
- [24] Chou K F and Dennis A M 2015 *Sensors-Basel* **15** 13288
- [25] Clapp A R, Medintz I L and Mattoussi H 2006 *Chemphyschem* **7** 47
- [26] Kholmicheva N, Moroz P, Eckard H, Jensen G and Zamkov M 2017 *Acs Energy Lett.* **2** 154
- [27] Kozawa D, Carvalho A, Verzhbitskiy I, Giustiniano F, Miyauchi Y, Mouri S, Neto A H C, Matsuda K and Eda G 2016 *Nano Lett.* **16** 4087
- [28] Achermann M, Petruska M A, Crooker S A and Klimov V I 2003 *J. Phys. Chem. B* **107** 13782
- [29] Becker K, Lupton J M, Muller J, Rogach A L, Talapin D V, Weller H and Feldmann J 2006 *Nat. Mater.* **5** 777
- [30] Borys N J, Walter M J, Huang J, Talapin D V and Lupton J M 2010 *Science* **330** 1371
- [31] Chen C W, Wang C H, Chen Y F, Lai C W and Chou P T 2008 *Appl. Phys. Lett.* **92** 051906
- [32] Chen Z Y, Berciaud S, Nuckolls C, Heinz T F and Brus L E 2010 *Acs Nano* **4** 2964
- [33] Crooker S A, Hollingsworth J A, Tretiak S and Klimov V I 2002 *Phys. Rev. Lett.* **89** 186802
- [34] Hua Z, Xu Q F, Huang X N, Zhang C F, Wang X Y and Xiao M 2014 *Acs Nano* **8** 7060
- [35] Wang C H, Chen C W, Wei C M, Chen Y F, Lai C W, Ho M L and Chou P T 2009 *J. Phys. Chem. C* **113** 15548
- [36] Yu J H, Sharma M, Sharma A, Delikanli S, Demir H V and Dang C 2020 *Light-Sci. Appl.* **9** 27
- [37] Zhang Q, Atay T, Tischler J R, Bradley M S, Bulovic V and Nurmikko A V 2007 *Nat. Nanotechnol.* **2** 555
- [38] Zhu H M, Yang Y, Wu K F and Lian T Q 2016 *Ann. Rev. Phys. Chem.* **67** 259
- [39] Shen H B, Wang H Z, Tang Z J, Niu J Z, Lou S Y, Du Z L and Li L S 2009 *Crystengcomm* **11** 1733
- [40] Medintz I L, Clapp A R, Mattoussi H, Goldman E R, Fisher B and Mauro J M 2003 *Nat. Mater.* **2** 630
- [41] Clapp A R, Medintz I L, Mauro J M, Fisher B R, Bawendi M G and Mattoussi H 2004 *J. Am. Chem. Soc.* **126** 301
- [42] Bockelmann U and Egeler T 1992 *Phys. Rev. B* **46** 15574
- [43] Klimov V I, Mikhailovsky A A, McBranch D W, Leatherdale C A and Bawendi M G 2000 *Science* **287** 1011
- [44] Robel I, Gresback R, Kortshagen U, Schaller R D and Klimov V I 2009 *Phys. Rev. Lett.* **102** 177404
- [45] Cragg G E and Efros A L 2010 *Nano Lett.* **10** 313
- [46] Bae W K, Park Y S, Lim J, Lee D, Padilha L A, McDaniel H, Robel I, Lee C, Pietryga J M and Klimov V I 2013 *Nat. Commun.* **4** 2661
- [47] Efros A L and Rosen M 1997 *Phys. Rev. Lett.* **78** 1110
- [48] Galland C, Ghosh Y, Steinbruck A, Sykora M, Hollingsworth J A, Klimov V I and Htoon H 2011 *Nature* **479** 203
- [49] Galland C, Ghosh Y, Steinbruck A, Hollingsworth J A, Htoon H and Klimov V I 2012 *Nat. Commun.* **3** 908
- [50] Rogez B, Yan H, Le Moal E, Leveque-Fort S, Boer-Duchemin E, Yao F, Lee Y H, Zhang Y, Wegner K D, Hildebrandt N, Mayne A and Dujardin G 2014 *J. Phys. Chem. C* **118** 18445
- [51] Ito Y, Matsuda K and Kanemitsu Y 2007 *Phys. Rev. B* **75** 033309
- [52] Ito Y, Matsuda K and Kanemitsu Y 2009 *Phys. Status Solidi C* **6** 221